Flexible Multiferroic Bulk Heterojunction with Giant Magnetoelectric Coupling *via* van der Waals Epitaxy

Tahta Amrillah,[†] Yugandhar Bitla,[‡] Kwangwoo Shin,[§] Tiannan Yang,[⊥] Ying-Hui Hsieh,[‡] Yu-You Chiou,[‖] Heng-Jui Liu,[Δ] Thi Hien Do,[#] Dong Su,[□] Yi-Chun Chen,[‖] Shien-Uang Jen,[#] Long-Qing Chen,[⊥] Kee Hoon Kim,[§] Jenh-Yih Juang,[†,] and Ying-Hao Chu[†,‡,#,○,*]*

[†]Department of Electrophysics and [‡]Department of Materials Science and Engineering, National Chiao Tung University, Hsinchu 30010, Taiwan, [§]CeNSCMR, Department of Physics and Astronomy, Seoul National University, Seoul 151-747, Republic of Korea, [⊥]Department of Materials Science and Engineering, Pennsylvania State University, University Park, Pennsylvania 16802, United States, [‖]Department of Physics, National Cheng Kung University, Tainan 70101, Taiwan, [Δ]Department of Materials Science and Engineering, National Chung Hsing University, Taichung 40227, Taiwan, [#]Insitute of Physics, Academia Sinica, Taipei 11529, Taiwan, [□]Center for Functional Nanomaterials, Brookhaven National Laboratory, Upton, New York 11973, United States, [○]Material and Chemical Research Laboratories, Industrial Technology Research Institute, Hsinchu 31040, Taiwan.

SUPPLEMENTARY INFORMATION

Table S1, summarizes the Raman shift of the phonon mode of BFO in BFO-CFO/mica, showing that the A_{1g} mode is shifted to the lower wavenumber in comparison with the result from BFO-CFO/STO indicating a weak enforce from mica substrate release the OOP strain of BFO pillars.[1] In contrast, a low wavenumber shift of the phonon modes of CFO (A_{1g} and T_{1g} modes) describes an increasing of its OOP tensile strain.[1-3] On the other hand, the phonon modes of CFO also shift to high wavenumber (E_g, T_{1g}, A_{1g} modes) which might be indicate any releasing of OOP strain by mica substrate.[1] The distortion of CFO crystal structure might be unstable under the influence of defects or BFO pillars embedded in the CFO matrix which may affect the distribution and symmetry of octahedral and tetrahedral sublattices of spinel CFO, thus, CFO phonon modes are varied and shift to lower and higher wavenumbers under constraint.

Table S1. The peaks of Raman spectrum indicates each BFO and CFO modes

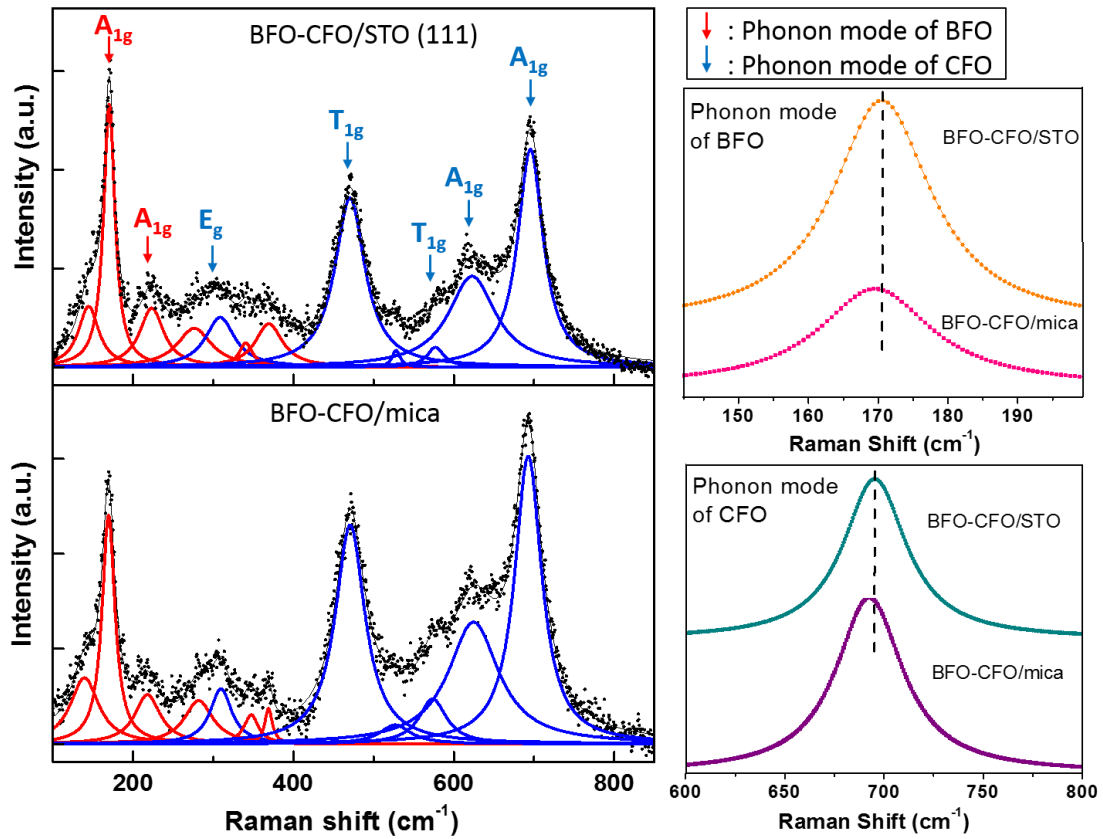|	mode	BFO-CFO/mica(cm^{-1})	BFO-CFO/STO(cm^{-1})
BFO	A_{1g}	169.59	170.52
	A_{1g}	218.17	223.43
CFO	E_g	309.74	308.73
	T_{1g}	470.72	470.44
	T_{1g}	573.6	577.06
	A_{1g}	624.46	622.63
	A_{1g}	692.63	695.34

Figure S1. Raman spectroscopy of BFO-CFO/mica and BFO-CFO/STO shows slightly different Raman shift due to different strain states imposed by mica and STO substrates.

The spectroscopy mapping of PFM exhibits a contrast of electric polarization switching of BFO pillars shown in red/yellow color signals, while CFO matrix shown in blue color signals. The piezo-response signal of BFO pillars is suppressed *via* strain coupling with the CFO matrix when the 2000 Oe magnetic field is applied (right hand side). This further confirm of the strong magnetoelectric *via* structural coupling between CFO matrix and BFO pillars.
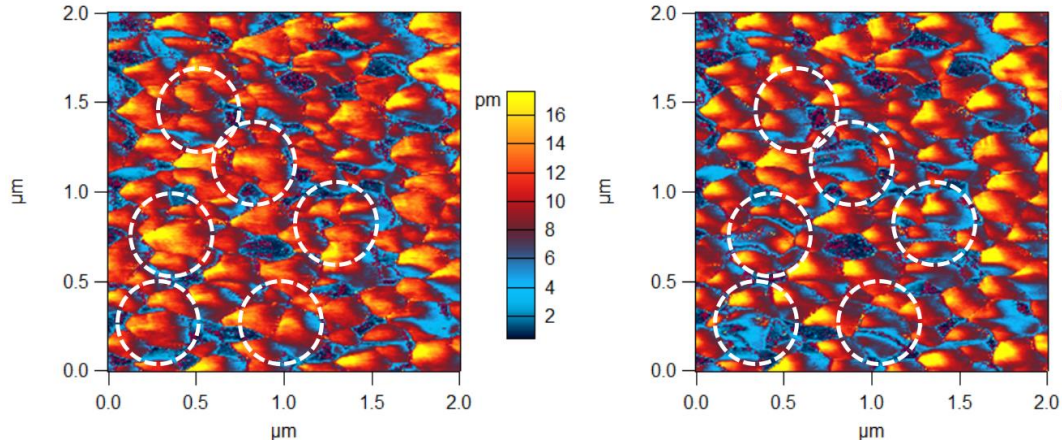
Figure S2. The PFM mapping with spectroscopy of BFO-CFO/mica. The contrast (red/yellow) indicates a piezo-response of BFO pillars has changed with an applied magnetic field of 2000 Oe (right hand side).

The piezoresponse of BFO-CFO/mica is small at the below room temperature because at low temperatures, electrons movement is slow and lattice vibrations are small, as well. Thus, the applied AC voltage cannot induce maximum elongation of the lattice in the PFM measurement. This is also reflected in the decreasing of the magnetoelectric coupling with decreasing temperature.
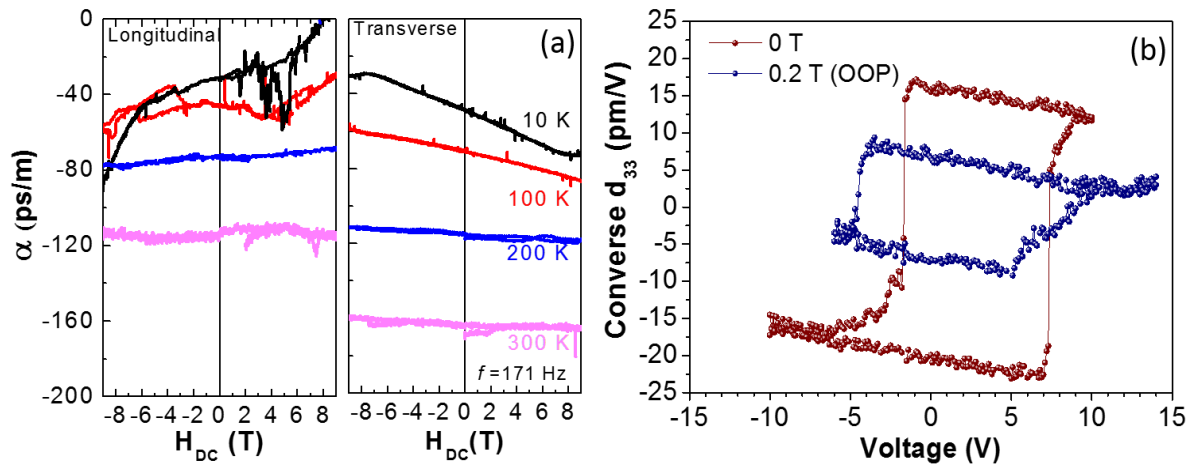
Figure S3. (a) Macroscopic and (b) Microscopic magnetoelectric measurement of BFO-CFO/mica at low temperatures.

The transversal MES (α_{31}) as the variation of bending radius is further tested, the α_{31} remains even under a small bending radius of 5 mm as shown in Figure S4. A permanent damage of the sample at the bending radius of 4 mm can be detected when the magnetoelectric coupling behavior vanishes.
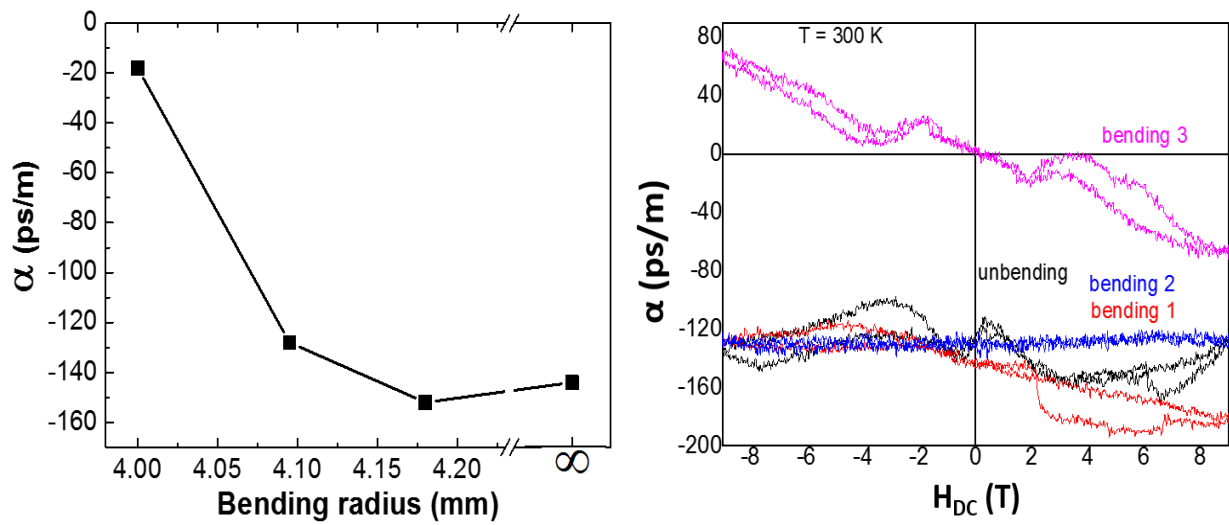

Figure S4. The transversal macroscopic magnetoelectric measurement of BFO-CFO/mica at various bending conditions.

The microscopic magnetoelectric measurements for various bending cycles under a bending radius of ~7 mm have been carried out to check the recoverability of ME coefficient as displayed in Figure S5. Top panel shows α_{ME} as a function of bending cycles calculated from the converse d_{33} (bottom panel) with and without magnetic field. The result shows a small variation of the α_{ME} up to 1000 bending cycles indicating that the ME coupling of this system is robust against mechanical bending.
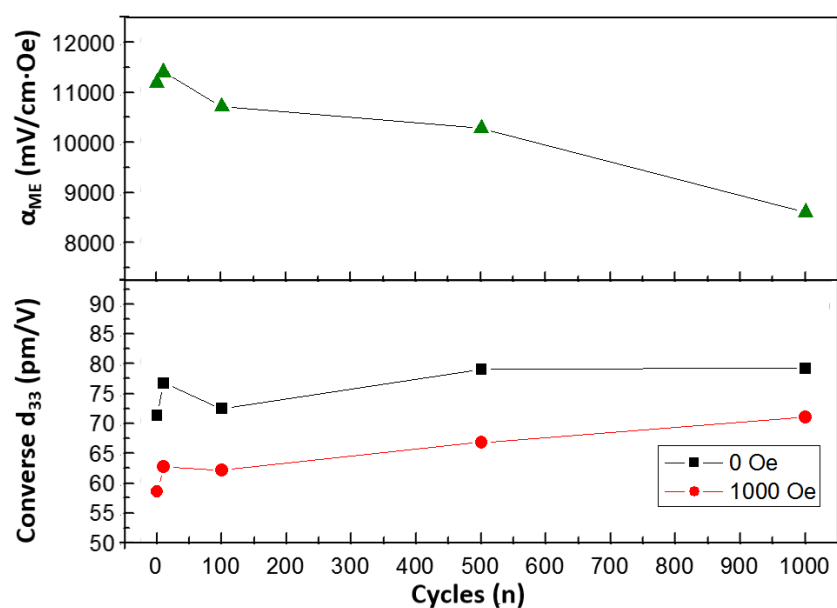
Figure S5. The microscopic α_{ME} in various bending cycles (top panel) calculated from converse d_{33} with and without magnetic field (bottom panel).

REFERENCES AND NOTES

1. Zhang, J.; Fu, H.; Lu, W.; Dai, J.; Chan, H. L. W. Nanoscale Free-Standing Magnetoelectric Heteropillars. *Nanoscale* **2013,** 5, 6747-6753.

2. Chaix-Pluchery, O.; Cochard, C.; Jadhav, P.; Kreisel, J.; Dix, N.; Sanchez, F.; Fontcuberta, J. Strain Analysis of Multiferroic $BiFeO_3$–$CoFe_2O_4$ Nanostructures by Raman Scattering. *Appl. Phys. Lett*. **2011,** 99, 072901.

3. Liao, Y. Y.; Li, Y. W.; Hu, Z. G.; Chu, J. H. Temperature Dependent Phonon Raman Scattering of Highly *a*-axis Oriented $CoFe_2O_4$ Inverse Spinel Ferromagnetic Films Grown by Pulsed Laser Deposition. *Appl. Phys. Lett*. **2012,** 100, 071905.